WD/ST/82/14 December 1982

An aquifer thermal energy storage experiment in the Lower Greensand at the IGS research site, Reach, Cambridgeshire

by

B. Adams M.Sc., M.I.Geol.

CONTENTS

LIST OF FIGURES

19. Temperature as a function of time in BA/R/2 (13 m from injection bore) during storage phase

20. Temperature as a function of time in BA/R/3 (5 m from injection bore) during storage phase

21. Temperature profiles in BA/R/1 (10 m from injection bore) during abstraction phase

22. Temperature profiles in BA/R/2 (13 m from injection bore) during abstraction phase

23. Temperature profiles in BA/R/3 (5 m from injection bore) during abstraction phase

24. Temperature as a function of time in BA/R/1 (10 m from injection bore) during abstraction phase

25. Temperature as a function of time in BA/R/2 (13 m from injection bore) during abstraction phase

26. Temperature as a function of time in BA/R/3 (5 m from injection bore) during abstraction phase

27. Temperature of abstracted water at well head as a function of time

28. Energy recovered as a function of the proportion of the volume of injected water recovered

29. Energy recovered as a function of time

30. Energy recovered as a function of well-head temperature

31. First cycle recovery factor versus cycle length for several injection-storage-rest schedules for three thermal volumes (after Doughty et al. 1982)

A1 Temperature of water in the injection borehole above the packer

An aquifer thermal energy storage experiment in the Lower Greensand at the IGS research site, Reach, Cambs.

1. INTRODUCTION

The storage of thermal energy in the form of heated water in aquifers has been discussed widely in the literature (see the reference lists in Adams et al. 1980; Meyer and Hausz, 1980; Schaetzle et al.1980) and several experimental studies have been carried out in this field. Indeed, aquifer thermal energy storage has been practised in China since 1965 (Qi-Sen Yan, 1981). Adams et al. (1980 and 1981) reported a need for preliminary experimental field studies to evaluate the potential of aquifer thermal energy storage (ATES) in the United Kingdom. Adams et al. (op. cit.) concluded that the Lower Greensand aquifer in the Cambridge area and the Permo-Triassic sandstones of the Midlands were apparently suitable for such experimental studies. This report describes an experiment carried out by the Hydrogeology Unit of the Institute of Geological Sciences using the Lower Greensand aquifer at Reach, near Cambridge, as the target aquifer.

The objectives of this experiment can be summarised as follows:

(a) To provide first hand experience of ATES field experimental procedures to aid future planning of more extensive ATES work.

(b) To demonstrate the Unit's interest and competence in ATES to potential funding agencies.

(c) To provide field data to be used for the calibration of an existing numerical model and, if necessary, development of further models.

The following constraints were placed on the experiment:

(a) Time

A considerable amount of work on the study of ATES had been carried out in USA and China and to a lesser extent France, West Germany, Switzerland, Japan, Denmark and Sweden (Adams et al. 1980). At the time of planning of the experiment the only published work in the UK relating to ATES had been carried out by IGS (Adams et al. 1981; Day et al. 1980). In order that IGS should maintain their advantage over other research organisations it was important to commence a field experiment as soon as possible to achieve the objectives listed above.

(b) Cost

It was evident that experimental costs should be kept to a minimum due to the financial climate. This would obviously limit the extent of the experiment.

2. EXPERIMENTAL DETAILS

The research site is located near the village of Reach 12 miles north east of Cambridge (NGR TL 558 659). Here the Lower Greensand aquifer is approximately 13 m thick underlain by Jurassic Clay and confined by 31.5 m of Gault Clay which in turn is overlain by about 4 m of Chalk. Four boreholes were drilled to penetrate the Lower Greensand - their relative locations are shown in Fig. 1 and their completion is fully described by Adams (1981).

The boreholes were completed using Demco Terraline 110 and Terrascreen which has a spcecified operating temperature range of $-10^{o}C$ to $+110^{o}C$, is non-corrodible in agressive groundwater and has complete resistance to regenerative chemicals. The major consideration for using thermoplastic casing and screen was its lower heat conductance as compared to metal casing (0.22 watts/m/deg C).

Borehole instrumentation was achieved by using probes constructed from 6 m lengths of 1 in. ABS plastic pipe (again chosen for its thermal characteristics) connected by flanged joints. Over the screened section of the borehole thermistors were mounted at 1 m intervals separated by neoprene washers (located by a flange) of slightly larger diameter than the casing - see Fig. 2. The thermistors used were YSI 44033 thermistors manufactured by the Yellow Springs Instrument Co. The purpose of the neoprene washers was to cut down convenction effects within the boreholes. In the Auburn experiment (Molz et al. 1979) convection proved significant and was controlled by backfilling each observation well within the thermal radius of influence with a clean medium sand. The advantage of the technique employed to control convection at Reach over that used at Auburn is that both the instrument strings and the wells can easily be recovered. A pressure transducer was also mounted on each probe. Additionally in the central borehole (the injection/abstraction borehole) an inflatable packer was inserted above the top of the aquifer - see Fig. 3.

Data logging was achieved by the use of an Apple II Microcomputer and four Kratos "Analog Link On" units. This system was operated by software written specifically for the experiment (Adams, 1982) and some minor additional hardware permitted a flexible means of data collection, storage and analysis. The system could also be programmed to provide digital outputs which could be used to control the experiment (by shutting or opening valves or switching pumps on or off when specified conditions were met); in practice this facility proved to be unnecessary. Additionally a backup power supply was provided to enable the computer to operate normally in the event of mains power failure and an alarm system was included which would telephone IGS headquarters in the event of a systems crash.

The hot water for injection was produced by three liquid propane gas boilers connected in parallel fed from a storage tank filled by groundwater from the Chalk aquifer. A lagged hot water storage tank was connected in line immediately after the boilers and water was injected down the borehole from this tank by use of a small pump. The hot water tank was necessary both to act as an air trap in an attempt to prevent the injection of gas into the aquifer, and to act as a stabilisation reservoir - the potential injection rate differing from the combined production rates of the reservoirs. Flow regulation valves were used and flow was measured by one flow meter upstream of the boilers and one downstream of the hot water storage tank. The meter on the cold water feed pipe also had a contact head counter which was used to transmit flow data to the computer. Float switches in both storage tanks were used to control the boiler feed and injection pumps. Thermistors were mounted at the well head and above the packer to monitor the temperature of the injected water and the temperature of the column of water above the packer. The system is shown in Fig.4.

The experiment involved a 279 day injection-storage-recovery cycle. Following sporadic injection tests over a period of a few days (in order to check equipment) full injection commenced on 24.2.82 and continued until 13.5.82 with only a few minor interruptions due to equipment failure in the early stages - a total of 77 days. An average injection rate of 19.74 m^3/day resulted in a total injection volume of 1520 m^3. Fig. 5 shows the cumulative injection volume as a function of time and Fig. 6 the injection temperature as a function of time - reasons for major variations in injection temperature are discussed in the following section. A 105-day storage period began on 13.5.82 and was terminated on 26.8.82 when abstraction of water from the Lower Greensand commenced. The abstraction phase continued for 97 days at an average rate of 20.21 m^3/day. Fig. 7 shows the cumulative abstraction volume as a function of time.

3. EXPERIMENTAL PROBLEMS

3.1 Thermistor Failure

By the end of the injection phase all of the thermistors mounted below the packer in the injection borehole had failed, thus preventing analysis of the temperature profile at the injection point. Molz and Melville (In Chang (Ed), 1982) report similar thermistor failure in the ATES experiment at Mobile, Alabama. They concluded that "the problem was chemical in nature, probably due to unexpectedly rapid water migration through the epoxy barrier used to isolate the thermistor from the surrounding groundwater. Evidently, such migration is significantly accelerated by temperatures above 60 ^{o}C". Only three thermistors failed, apart from the 8 in the injection borehole out of a total of 45 in the whole of the Reach experiment and, apart from within the injection borehole, borehole temperatures were significantly lower than 60 ^{o}C.

3.2 Injection Temperature Fluctuation

Injection was stopped on days 7 and 8 in order to change the pressure transducer below the packer in the injection borehole. This resulted in a decrease in the temperature recorded by the well head thermistor (see Fig. 6), although it should be noted that no injection actually occurred at this temperature. The increase in injection temperature at day 28 (see Fig. 6) was caused by the installation of improved regulator valves which permitted finer balancing of individual boilers. Failure of one of the boilers caused the temperature decrease recorded at day 38 and its replacement by a new boiler resulted in an improved temperature from day 43 onwards.

3.3 Leakage of Injection Water into the Injection Borehole Above the Packer

During the testing period prior to the main injection period problems were encountered with the use of the packer. On initial injection tests the packer split and the combination of partial deflation of the packer and the introduction of nitrogen gas (used for inflating the packer) into the column of water above the packer caused water to rise within the injection borehole - for this reason a float switch was inserted into the top of the injection borehole which, if activated, would switch off the injection pump. Once the packer had been repaired it was resited just above the top of the aquifer, however on initiating injection, water once again rose in the borehole above the packer. Repeated testing of the packer and logging of the borehole under injection and static conditions using a temperature/conductivity probe and down the hole TV failed to positively identify the cause. However the problem was solved by raising the packer to be central within the next section of casing. It is assumed that cavities in the Gault Clay immediately behind the casing had not filled by natural slumping and that injected water was rising up behind the casing and re-entering the injection borehole at the next casing joint upwards. If the casing joints above the suspect joint had greater integrity then repositioning the packer in the next length of casing upwards would prevent the leakage - as was the result.

3.4 Possible leakage of injection water into the Chalk aquifer

Although resiting the packer prevented the injection water leaking back into the borehole above the packer it was still possible that injection water was leaking to the Chalk aquifer by migration vertically behind the casing. In order to investigate the possibility, a chalk observation borehole was located 1.05 m from the injection borehole in a direction approximately parallel to the hydraulic gradient, see Fig. 1 (this location was chosen as it was the closest possible to the injection bore). The borehole was instrumented with three thermistors (to monitor water temperatures at the top, middle and bottom of the saturated portion of the Chalk), and a Munro recorder to monitor variation in water level. Instrumentation was completed on 25.3.81 the 29th day of the injection

cycle. Fig. 8 shows the recorded increase in temperature within the Chalk observation borehole over the remainder of the injection period. The temperature difference over the column of water is due either to convection or preferential heat transference within the upper part of the aquifer or a combination of both. It was important to determine the cause for this rise in temperature; whether it was due to leakage of hot injection water or whether it could be accounted for by horizontal conduction through the Chalk from the hot column of water above the packer.

The rise in temperature within the Chalk observation borehole due to conduction of heat from the column of water above the packer in the injection borehole was calculated as approximately 9^{o}C - see Appendix A. It was therefore concluded that the recorded rise in temperature at the Chalk observation borehole could be explained by conduction of heat through the saturated Chalk and that the Gault Clay had sufficiently sealed against the casing, following well completion, to prevent leakage of water into the Chalk.

Additionally, the recorded water level on the Munro recorder showed no response attributable to the switching of the pump at the end of the injection phase nor at the commencement of abstraction.

3.5 Borehole clogging

A potential problem with aquifer thermal energy injection boreholes is clogging from one or more of the following: clogging by air entrapment or particulate deposition, chemical clogging and bio-chemical clogging. Problems relating to aquifer and borehole clogging have been discussed in the literature (Molz *et al*. 1979; Molz *et al*. 1981; Adams *et al*. 1980; Meyer and Hauz, 1980; Tsang (Ed) 1978; Yan, 1981). In the Reach experiment it was felt that as the total quantity of water to be injected was relatively small, expensive or complex provisions (such as treatment plant and backwashing facilities) could not be justified. However some consideration was given to the potential problem. Part of the reason for installing the hot water storage tank after the boilers was to act as an air trap to minimise injection of gas into the aquifer, and the cold water tank whilst acting as a reservoir for the boilers also acted as a settling tank to decrease particulate content of the injected water.

Chemical incompatibility of the Chalk and Lower Greensand waters was not felt to be a major problem. The initial Chalk-water would be saturated or oversaturated with respect to calcite, the solubility of which decreases with rising temperature. Depending on the kinetics of heating and injection system the calcite would precipitate out, probably in finely divided particulate form. As the Chalk-water cools, following injection, the solubility of calcite would increase which, coupled with the probability that the Lower Greensand aquifer contained high CO_2, would result in the re-solution of any remaining particulate $CaCO_3$. Additionally if the Lower Greensand were anoxic then the injection of aerated water

would create a redox front causing precipitation of iron (and possibly manganese). However, Van Beek (1980) has shown that such precipitation has no serious effect on aquifer permeability. Thus while deposition in the boilers, pipes and hot water tank may have been a potential problem it was felt that chemical clogging of the well and/or aquifer was not.

Biochemical clogging was assumed not to be a problem on such a short time scale.

3.6 Flow metering

As discussed earlier and shown in Fig. 4 water flow rates were monitored by a cold water meter between the boiler feed tank and the boilers and a hot water meter between the hot water tank and the injection borehole. These flow meters were read manually on each site visit but additionally a contact-head-closure-counter on the cold water meter permitted the microcomputer to continuously monitor the flow by recording the number of counts activated by the contact closure (1 counter per 100 litres). At the end of the period of injection the total flows recorded by the two flow meters were as follows)1520.0133 m^3 on the cold water meter and 1522.6297 m^3 on the hot water meter - a difference of 2.6 m^3. This difference is probably due to a combination of leakage in the system (minor problem) and inaccuracies in the meter readings due to their installation position not permitting sufficient length of straight pipework before and after the meters to prevent turbulence affecting the impellers. However the difference of 2.6 m^3 in 1520 is not significant (0.1%).

However the total flow as monitored by the flow counter is 1640.8 m^3. This significant difference is apparently due to the interface system used between the contact head and the Kratos "Link On". It would appear that the contacts on the uniselector unit, which is used in the interface, did not always set properly and could read less for one reading than the previous reading - the software for the data logging assumes this to be an increase of one revolution of the uniselector counter rather than a backwards movement. Although the uniselector unit would be self correcting in the next log, the software was such that the incorrect flow count had already been stored. Thus, although the data stored by the logging system can be used to show the trend of the water injection curve, the data collected manually from the flow meters should be used for calculation purposes.

4. RESULTS

Figs 9, 10 and 11 show vertical temperature profiles in the observation wells during the injection phase. There is no apparent evidence of convection within the storage formation, and the change in temperature of the profiles at the top of the aquifer (indicated by the dotted line) suggests that the neoprene separators, installed to inhibit convection, were generally effective. The peaks in the profiles for BA/R/1 and BA/R/2 may be due to variations in horizontal permeability with depth which, if present, in the direction of BA/R/3 was masked due to the close proximity of this bore to the hydrothermal source. Figs 12, 13 and 14 show the variation of temperature with time for single thermistors in these bores.

Figs 15, 16 and 17 show the temperature profiles in the three observation wells over the storage period. It can be seen that temperatures within boreholes BA/R/1 and BA/R/3 decline over this period whereas in borehole BA/R/2 (the furthest from the injection borehole) the temperature continues to rise. This pattern is shown more clearly in Figures 18, 19 and 20. Locally the hydraulic gradient within the Lower Greensand is in the direction from BA/R/2 to BA/R/4 and so the rising temperature noted in BA/R/2 is unlikely to be due to general movement of the injected plume of water away from the injected zone under the natural hydraulic gradient - but rather delayed response in BA/R/2 due to its further distance away from the injection borehole.

On initiation of the abstraction phase the rate of decrease of temperature noted in boreholes BA/R/1 and BA/R/3 is increased and the temperature rise in BA/R/2 reversed - see Figs 21-23 and 24-26. The abstraction rate was set as closely as possible to the injection rate. Fig. 27 shows the well head temperature as a function of time during the abstraction phase.

Using the recorded temperatures and flow rates of the injected and abstracted water as functions of time, the amount of thermal energy injected and recovered can be calculated. A finite difference approximation of expression (1) is made to give equation (2) (Molz et al. 1979).

$$E_{in} = \int_{t_2}^{t_1} \rho C \left[T_i(t) - T_a\right] I(t)\, dt \qquad (1)$$

$$E_{out} = \int_{t_2}^{t_3} \rho C \left[T_r(t) - T_a\right] R(t)\, dt$$

Where E_{in} is the energy injected

E_{out} is the energy recovered

ρ = water density

C = specific heat of water

$T_i(t)$ = temperature of injected water

$T_r(t)$ = temperature of recovered water

T_a = ambient groundwater temperature

$I(t)$ = injection rate

$R(t)$ = recovery rate

The limits t_0, t_1 and t_2, t_3 correspond to the time periods of injection and abstraction respectively.

$$E_{in} \simeq \frac{\bar{\rho} \cdot \bar{C}}{2} \sum_{n} [T_i(t_n) + T_i(t_{n+1}) - 2\,T_a] \quad (QI_{n+1} - QI_n)$$

$$E_{out} \simeq \frac{\bar{\rho} \cdot \bar{C}}{2} \sum_{m} [T_r(t_m) + T_r(t_{m+1}) - 2\,T_a] \quad (QR_{m+1} - QR_m) \qquad (2)$$

where QI is volume of water injected

QR is volume of water recovered

$\bar{\rho}$ is average ρ

$\bar{C}$ is average C

indices n and m correspond to times when temperature and cumulative injection or recovery data were recorded.

Using equation (2) it can be shown that a total of 86.64 M W Hrs energy was injected and a total of 28.19 M W Hrs abstracted - the total abstracted volume being greater than the injected volume by a factor of 1.29.

A thermal energy recovery factor can be defined as the ratio of total energy recovered (E_{out}) at any time during abstraction to total energy injected (E_{in}). Fig. 28 shows this ratio plotted as a function of time and Figs. 29 and 30 show this ratio plotted as a function of time and as a function of recovery temperature respectively.

It can be seen that a total of 32.5% of the energy injected was recovered for 129% of the volume injected. An energy recovery factor of 27% was achieved for 100% volume recovery factor.

5. DISCUSSION OF RESULTS

The figure of 32.5% for the energy recovery factor for a 129% water recovery factor (i.e. ratio of water abstracted to water injected) is lower than some figures achieved in previously published results of experiments and theoretical studies for a single injection-storage-recovery cycle in a confined aquifer - see Table 1. There are two main reasons for the relatively lower figure achieved in the Reach experiment: the relatively small volume of water injected and the relative thinness of the storage aquifer. For the one experiment where both these factors are smaller than at Reach the recovery factor is only 13.5% - see Table 1.

Due to financial constraints the total injected volume of water was relatively small (only 1520 m^3). Now, assuming a constant thickness of the aquifer and that the injected water occupies the aquifer in the shape of a cylinder any increase (or decrease) in the injected volume by a factor X is reflected by an increase (or decrease) in the curved surface area of the cylinder by a factor of $X^{\frac{1}{2}}$. Thus, assuming the major heat loss from the injected water is horizontally rather than vertically (i.e. through the curved surface area) then relative heat loss is greater the smaller the injected volume. Similarly, the thinner the aquifer the greater the curved surface area for any particular injection volume and so heat losses will be relatively greater the thinner the aquifer. Additionally the thinner the aquifer the higher the relative vertical losses (Sauty et al. 1982).

In a theoretical study on aquifer thermal behaviour (Doughty et al. 1982) showed that the recovery factor is a function of five dimensionless parameters:

$P_e = C_a R^2 / 2\lambda_a t_i$

$\Lambda = C_a^2 H^2 / C_c \lambda_c c t_i$

λ_a / λ_c

C_a / C_c

N

where

P_e is the Peclet number

C_a is the aquifer volumetric heat capacity

C_c is the confining layer volumetric heat capacity

λ_a is the aquifer thermal conductivity

λ_c is the confining layer thermal conductivity

R is the thermal radius

H is the aquifer thickness

t_i is the length of the injection cycle

N is the number of cycles

TABLE 1. Energy recovery factors from published ATES experiments and modelling exercises.

Reference	Aquifer thickness	Length of injection-storage-abstraction cycle	Quantity of water injected	Energy recovery factor
	(m)	(days)	(M^3)	(%)
Mobile experiment (Molz et al. 1979)	21.4	170	54800	65
Univ. of Yamagata expt (Yokoyama in Tsang (Ed) 1980)	19	64	9930	40
RISØ theoretical study (Reffstrup and Würtz 1979)	30	365	approx 87600 m^3	36
Texas A & M theoretical study (Schaetzle et al. 1980)	4.6	365	approx 30000	20
" "	7.6	365	" "	40
" "	15.2	365	" "	65
Bonnaud, Jura. (Sauty et al. 1982)	2.5	12	490	13.5
Reach, UK 1982	13	280	1520	32.5

Doughty et al. (op. cit.) in considering the recovery factor's dependence on P_e Λ and λ_a/λ_c showed that it is most sensitive to changes in these parameters at small values of P_e and Λ. Thus the recovery factor is significantly decreased for relatively small injection volumes, and relatively thin aquifers.

With regard to the relative duration of injection, storage, abstraction and rest phases, Doughty et al. (op. cit.) produced a set of curves for first cycle recovery factor as a function of the total cycle time for different schedules for three thermal volumes - see Fig. 31. In case A the fluid is injected during the first half of the cycle and produced during the second half - there being no storage or rest period. Case B refers to a cycle which is divided into equal injection, storage, production and rest periods. Case C consists of a hypothetical cycle with instantaneous injection and production. Thus, for a given injection-storage-recovery-rest cycle time t_c, the recovery factor is less for longer storage periods t_s. In the Reach experiment the storage period was 104 days compared to an injection period of 77 days.

In the light of these considerations it is understandable that the recovery factor achieved in the Reach experiment appears relatively low. However, it is evident that much of the "lost" heat energy will have gone to heating the aquifer matrix and that during any successive thermal energy storage cycles heat losses will decrease and then the heat recovery factor will increase.

However one of the major objectives in carrying out this experiment was to provide calibration data for a digital model. Once the model is calibrated it can then be used to predict performance figures for different aquifers. The model to be used will be the Conduction-Convection-Consolidation model or "CCC" developed at the Lawrence Berkeley Laboratory (Lippmann et al. 1977). Work is currently proceeding on making this model available on two separate mainframe computers accessible by this department and once this work is completed simulation of the Reach experiment can commence.

6. SUMMARY AND CONCLUSIONS

An experiment to investigate aquifer thermal energy storage has been successfully completed using the Lower Greensand at Reach, Cambridgeshire, as the storage aquifer. A total of 1520 m^3 of water was injected over a period of 78 days at a mean temperature of 57 ^oC. A storage period of 105 days was followed by an abstraction period of 97 days at the end of which recovery of 32.5% injected heat energy had been achieved. This comparatively low recovery factor is due to the relatively small injection volume used, the thickness of the target aquifer and the length of the storage period compared to the injection and recovery periods. It is evident that much of the unrecovered heat energy was dissipated in heating the aquifer matrix and so further injection cycles would result in higher recovery coefficients.

Data logging, storage and analysis were facilitated by the use of an Apple II microcomputer and the experience gained in this aspect alone should prove valuable to both research and resource projects in this department in the future.

Data from this experiment will be used to calibrate the "CCC" digital model which in turn will be used to indicate potential recovery factors both under different conditions and for further cycles of injection storage and recovery.

REFERENCES

Adams, B., Barker, J.A. et al. 1980. Thermal energy storage in permeable formations in the United Kingdom. WD/ST/80/2.

Adams, B., Kitching, R. et al. 1981. Investigation of the potential of aquifer thermal energy storage in the United Kingdom. Proceedings of the International Conference on Energy Storage - Brighton.

Adams, B. 1982. Programs for the Apple II microcomputer used for the ATES experiment at Reach and for subsequent data analysis. WD/ST/82/15.

Day, J.B.W., Black, J. et al. 1980. A physical model study of the storage of low grade heat in unsaturated Chalk. Internat. Geol. Congress, Paris.

Doughty, C., Hellström, G. et al. 1982. A dimensionless parameter approach to the thermal behaviour of an aquifer thermal energy storage system. Water Res. Res. Vol 18, No 3, pp 571-587.

Hantush, M.S. 1964. Hydraulics of wells. Advances in Hydroscience, Vol 1, pp 281-432.

Jaeger, J.C. 1956. Numerical values for the temperature in radial heat flow. J. Math. Phys. 34. pp 316-321.

Lippman, M.J., Tsang, C.F. et al. 1977. Analysis of the response of geothermal reservoirs under injection and production procedures. Soc. Petrol. Engineers Journ. SPE 6537.

Meyer, C.F. and Hausz, W. 1980. Guidelines for conceptual design and evaluation of aquifer thermal energy storage. Report for Pacific Northwest Laboratory STES Program. PNL 3581 UC 94e GE 80T MP-44.

Molz, F.J., Parr, A.D. et al. 1979. Thermal energy storage in a confined aquifer: Experimental results. Water Res. Res. 15 No 6, pp 1509-1514.

Molz, F.J., Parr, A.D. and Andersen, P.F. 1981. Thermal energy storage in a confined aquifer: Second cycle. Water Res. Res. 17 No 3, pp 641-645.

Molz., F.J. and Melville. 1982. STES Newsletter contribution. Vol IV No 2.

Qi-Sen Yan. 1981. The development and application of aquifer storage in China.
Proceedings of Int. Conf. on Energy Storage - Brighton.

Reffstrup, J. and Würtz, J. 1979. Seasonal heat storage in aquifers.
Int. Assembly on Energy Storage, Dubrovnik, Yugoslavia.

Sauty, J.P., Gringarten, A.C. et al. 1982. Sensible energy storage in aquifers. 2. Field experiments and comparison with theoretical results.
Water Res. Res. 18 No 2, pp 253-265.

Schaetzle, W.J., Brett, C.E. et al. 1982. Thermal Energy Storage in Aquifers. Published by Pergamon Press.

Tsang, C.F. (Editor). 1978. Thermal energy storage in aquifers workshop - proceedings.
Lawrence Berkeley Lab. Univ. California LBL-8431. NTIS (CONF-7805140).

Van Beek, C.G.E.M. 1980. A model for the induced removal of iron and manganese from groundwater in the aquifer.
Int. Assoc. Geochem. & Cosmochem. & Alberta Research Council. 3rd Int. Symp. on Water-Rock Interaction - Edmonton

Yokoyama in STES Newsletter. June 1980.

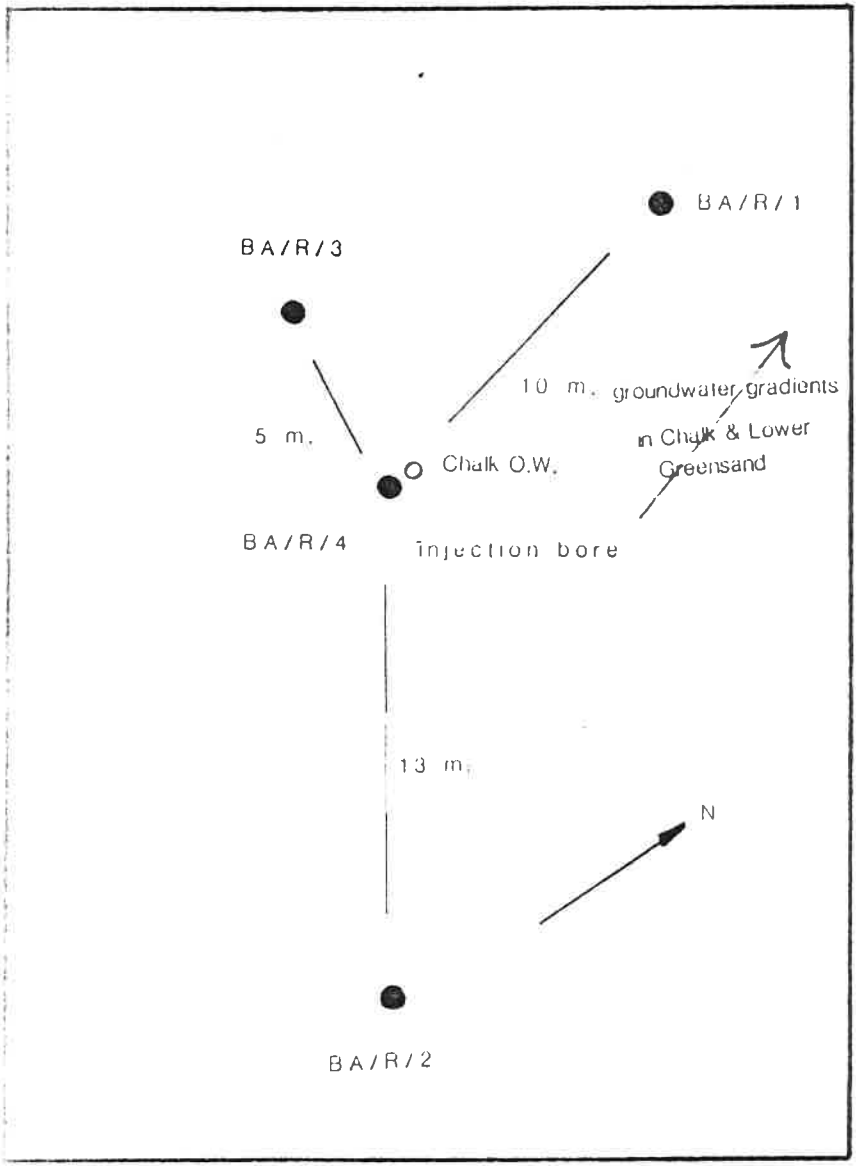

FIGURE 1.Relative borehole locations

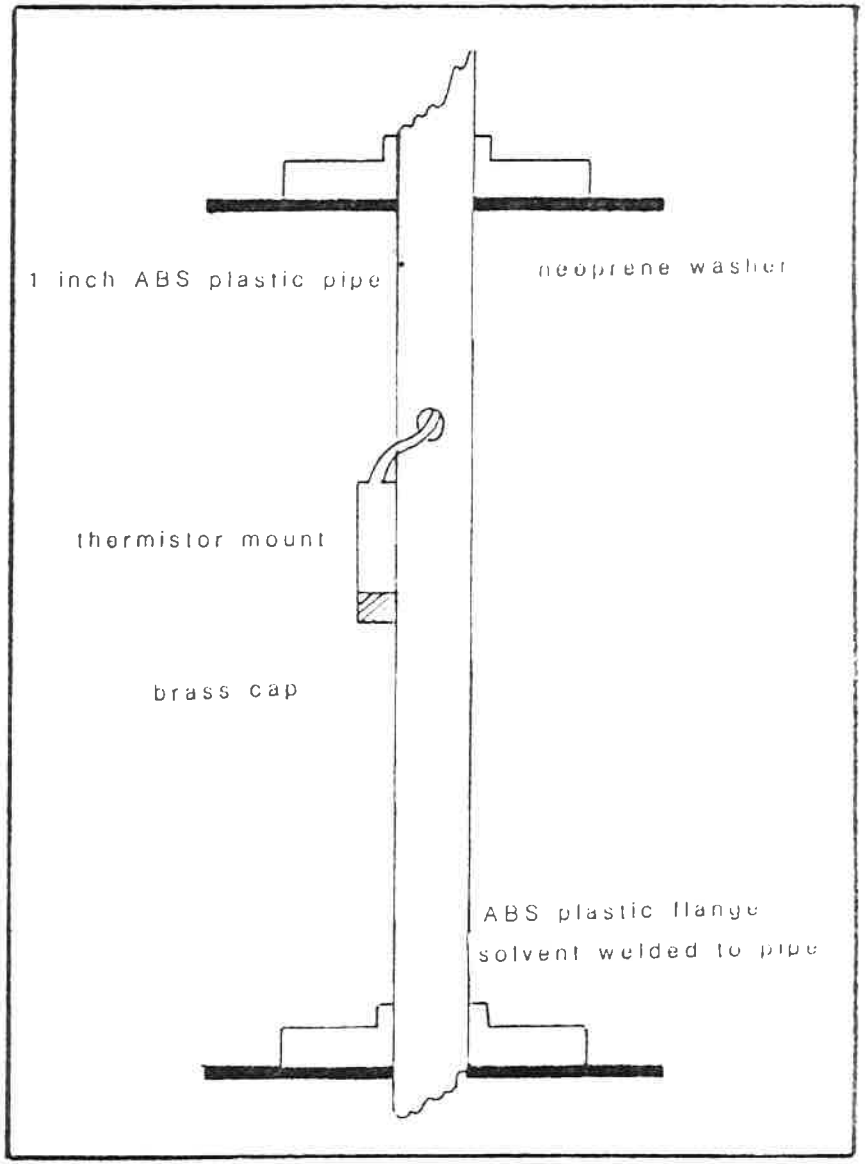

FIGURE 2.Instrumentation probe for borehole

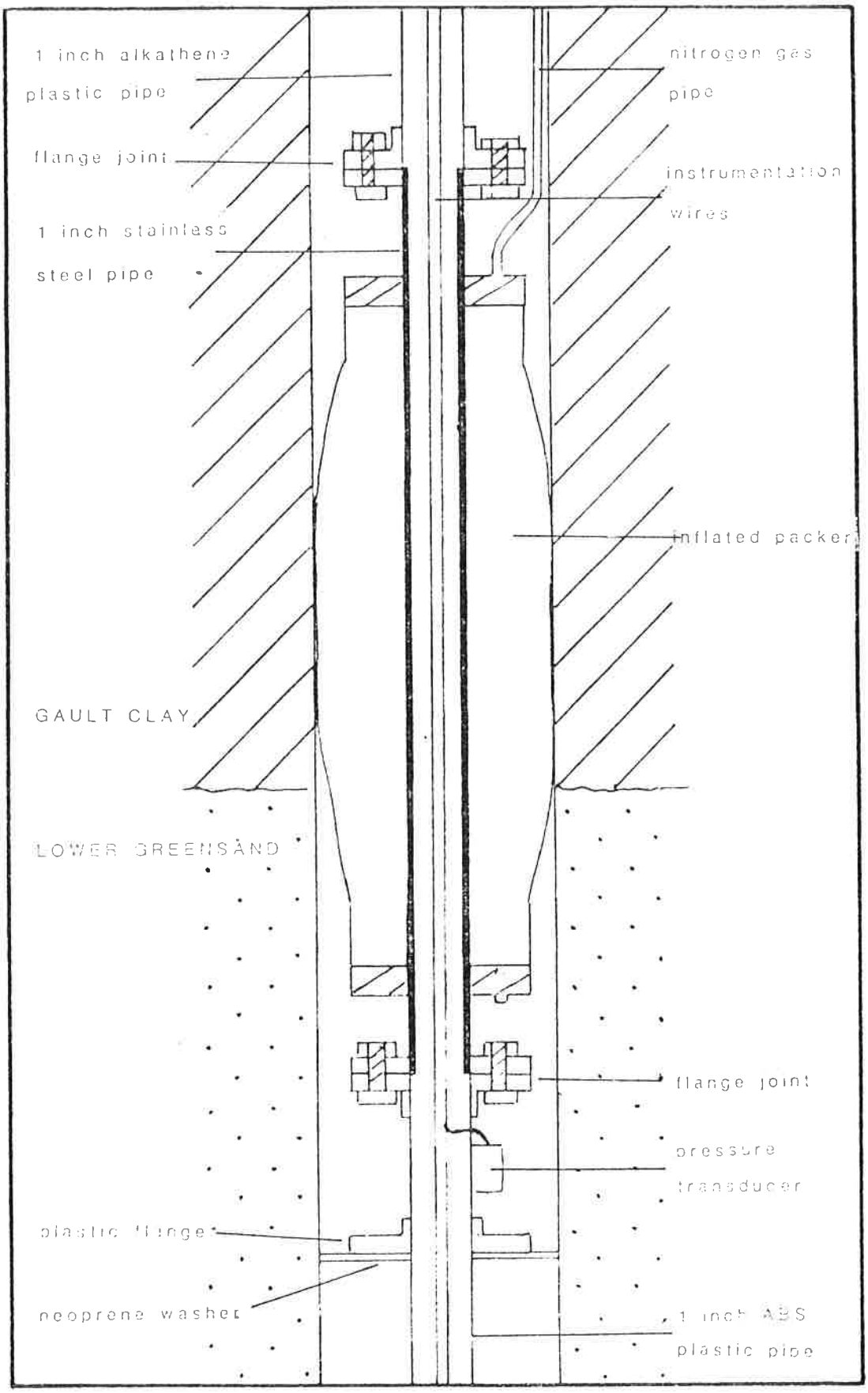

FIGURE 3. Inflatable packer positioned at top of aquifer in injection bore

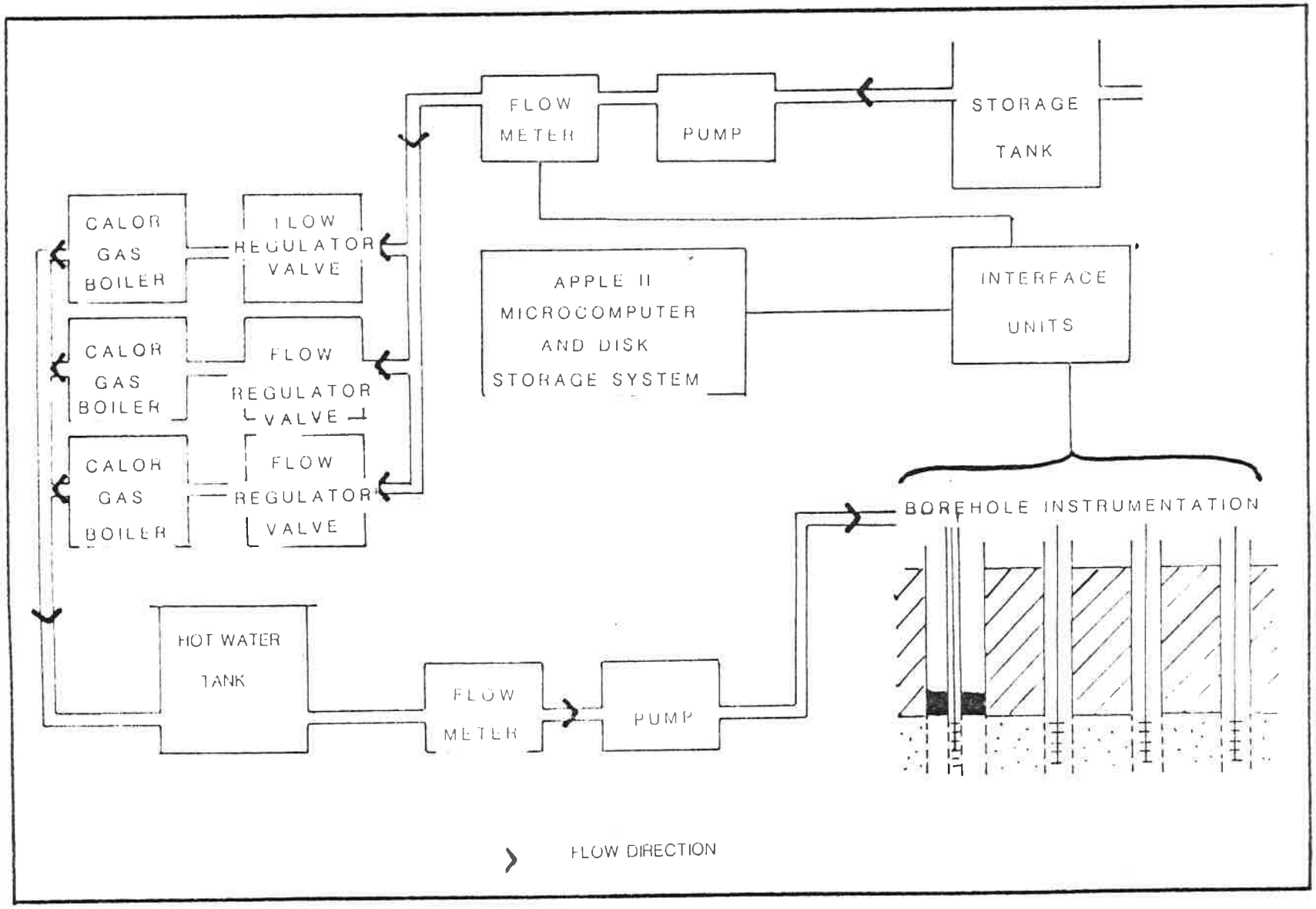

FIGURE 4. Schematic representation of experimental hardware (not to scale)

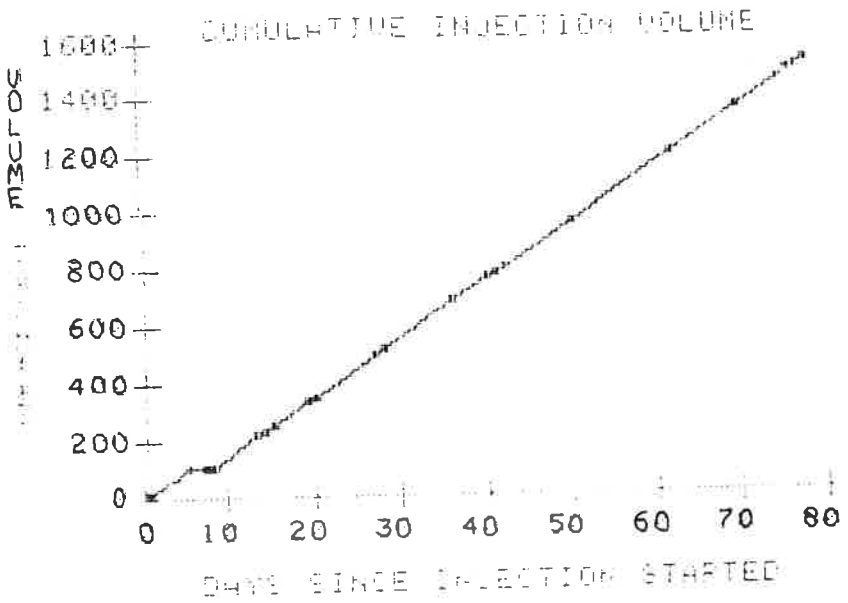

FIGURE 5. Injection volume as a function of time.

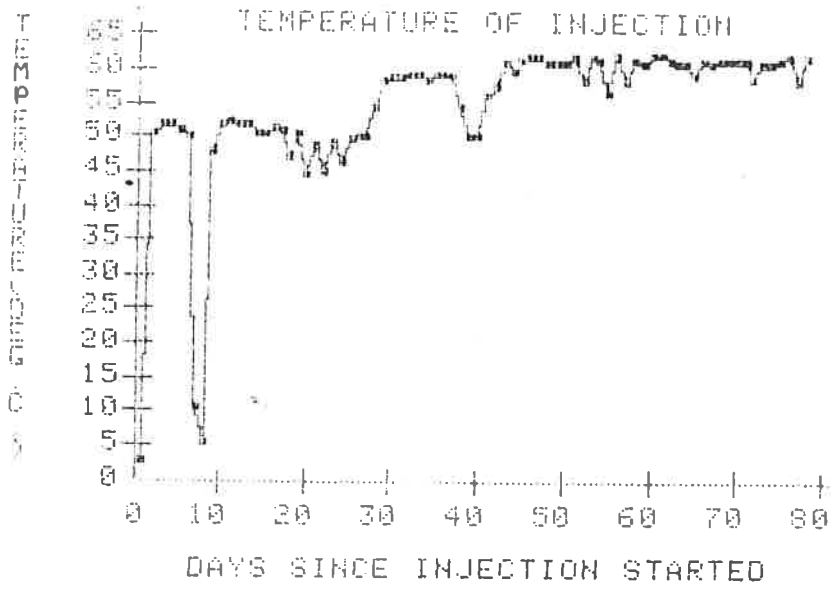

FIGURE 6. Injection temperature (at well head) as a function of time.

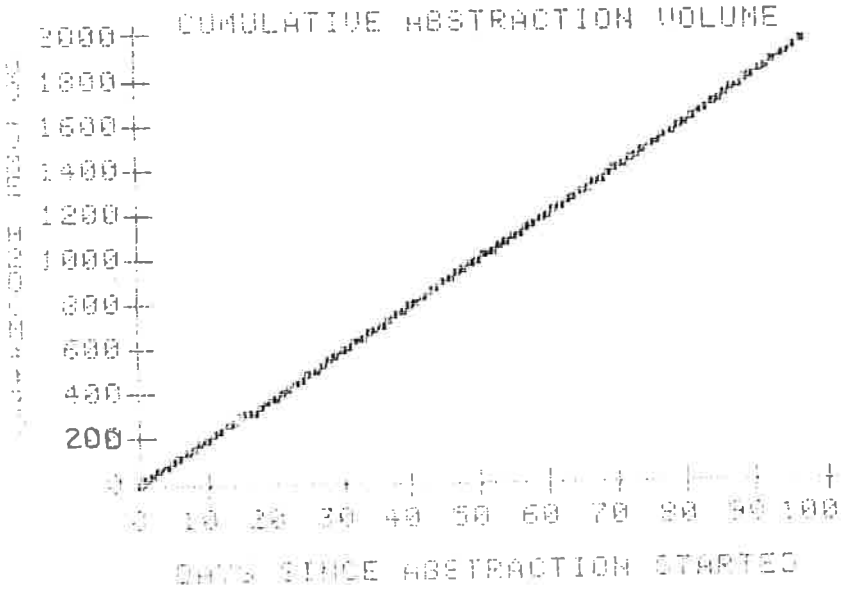

FIGURE 7. Abstraction volume as a function of time.

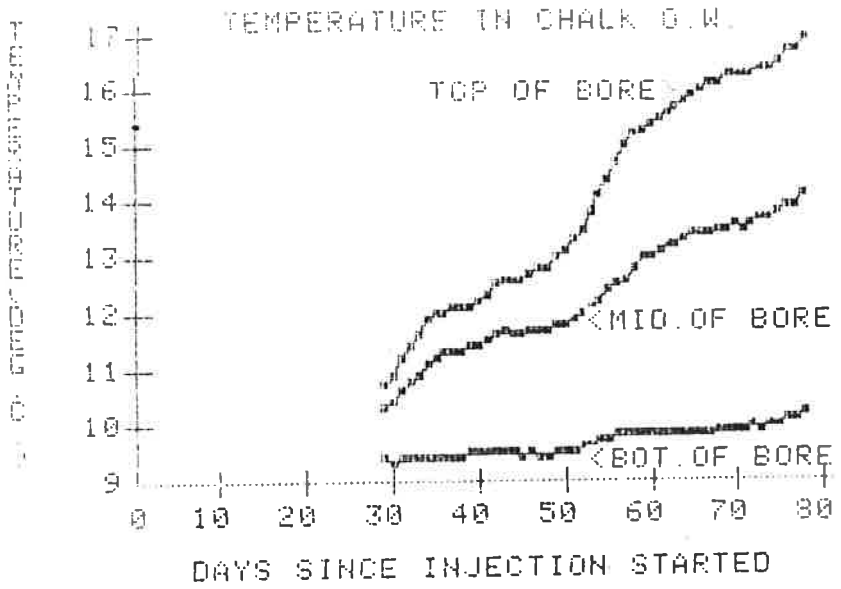

FIGURE 8. Recorded temperatures in Chalk observation borehole during injection phase.

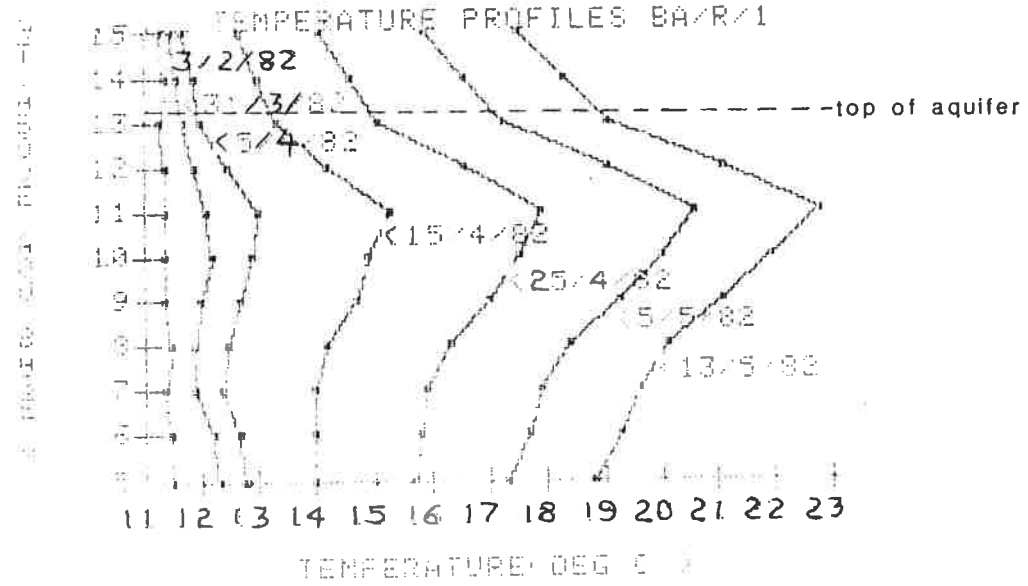

FIGURE 9. Temperature profiles in BA/R/1 (10 m from injection bore) during injection phase.

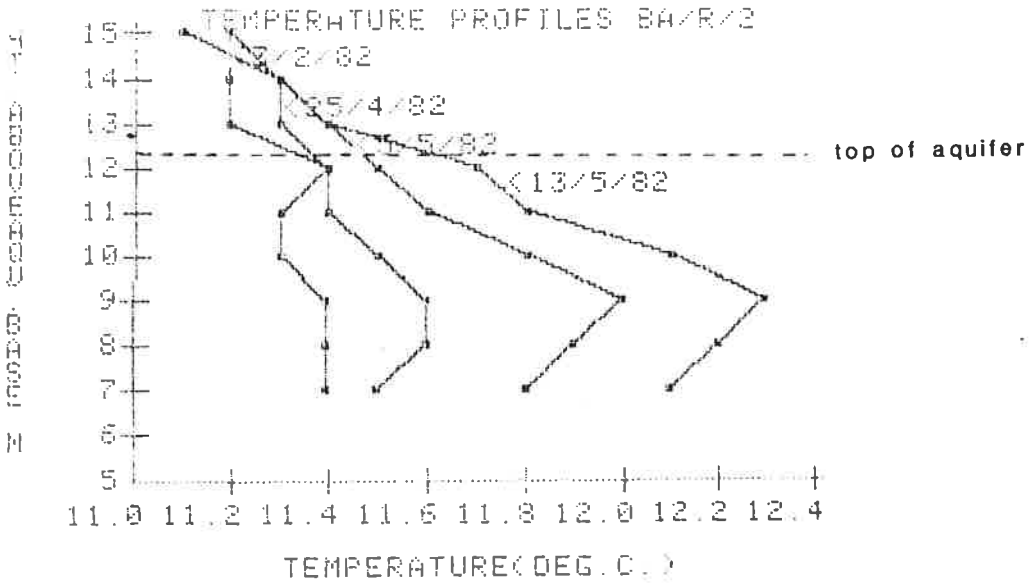

FIGURE 10. Temperature profiles in BA/R/2 (13 m from injection bore) during injection phase.

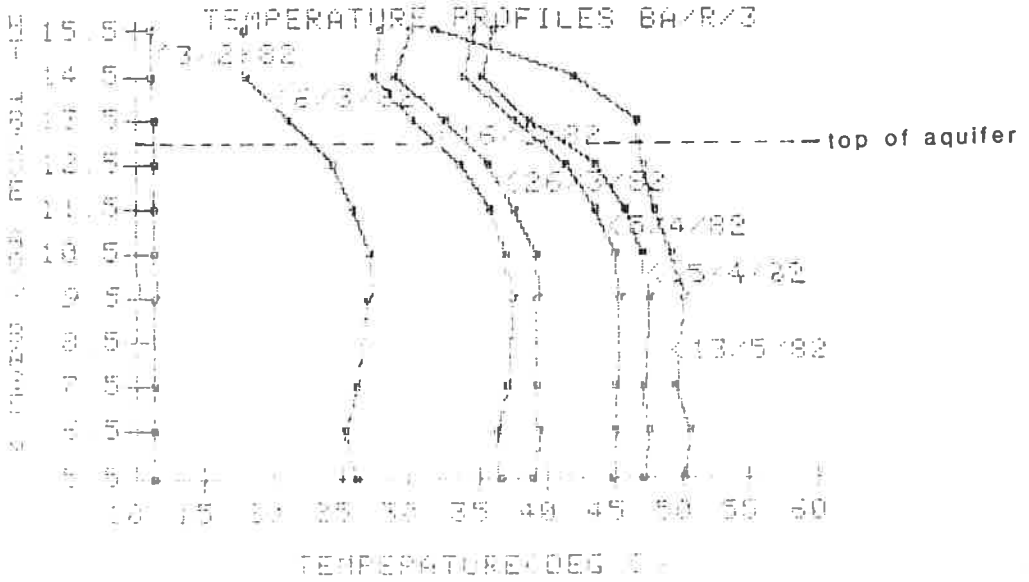

FIGURE 11. Temperature profiles in BA/R/3 (5 m from injection bore) during injection phase.

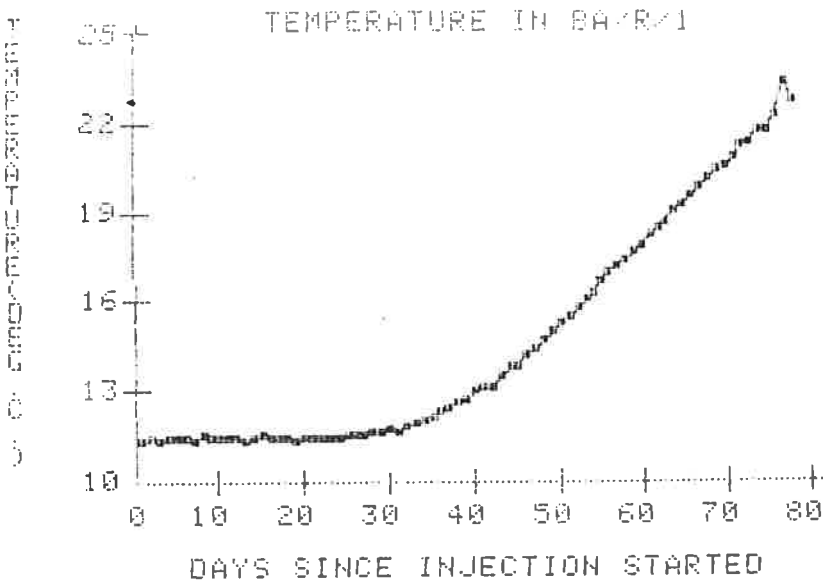

FIGURE 12. Temperature as a function of time in BA/R/1 (10 m from injection bore) during injection phase.

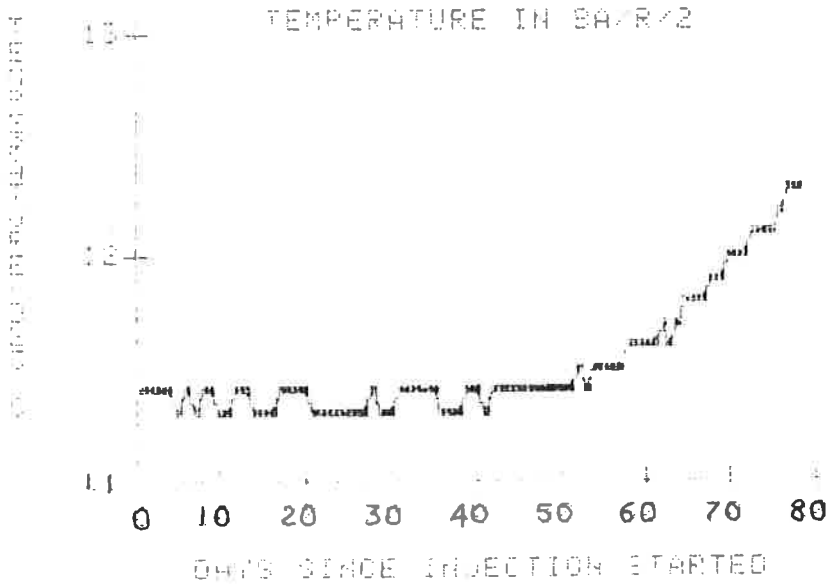

FIGURE 13. Temperature as a function of time in BA/R/2 (13 m from injection bore) during injection phase.

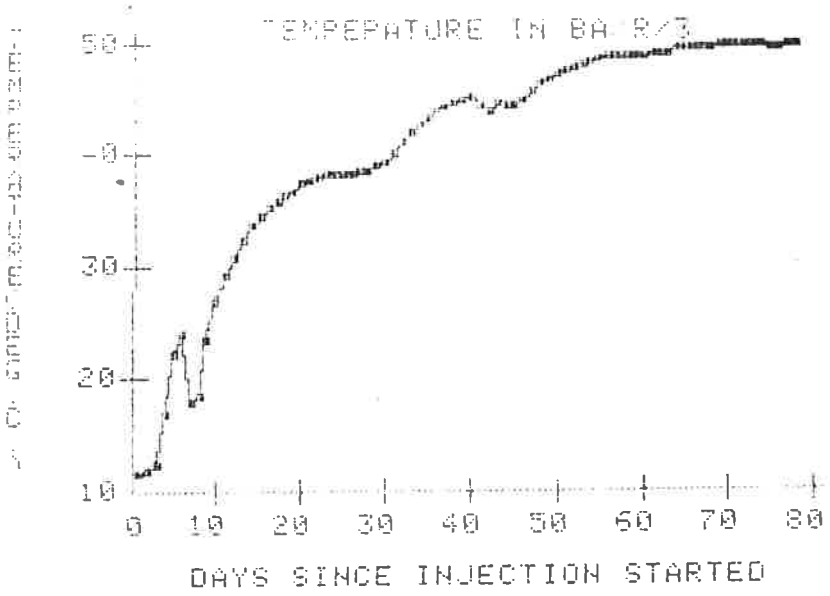

FIGURE 14. Temperature as a function of time in BA/R/3 (5 m from injection bore) during injection phase.

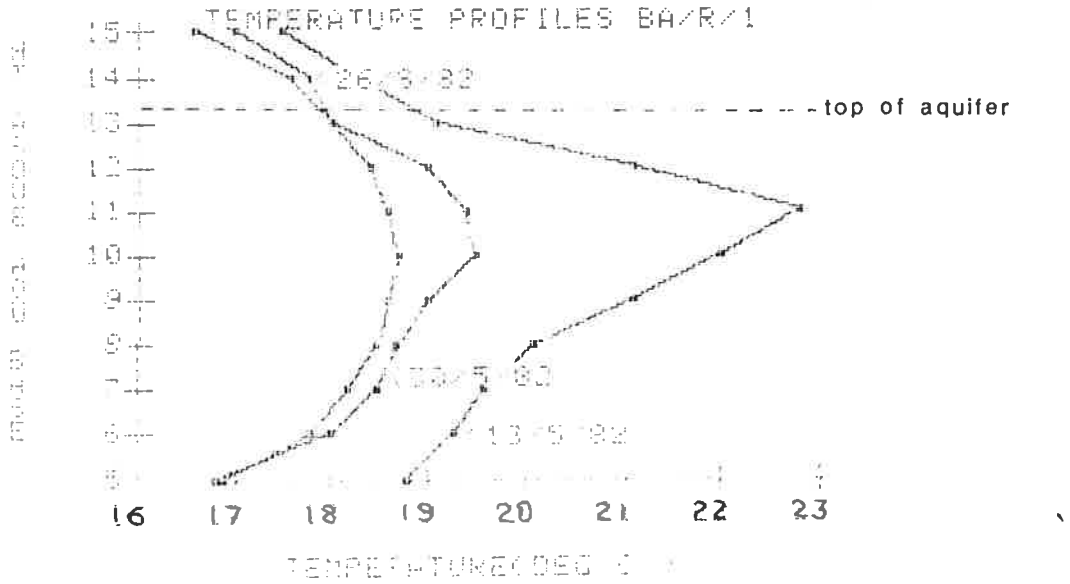

FIGURE 15. Temperature profiles in BA/R/1 (10 m from injection bore) during storage phase.

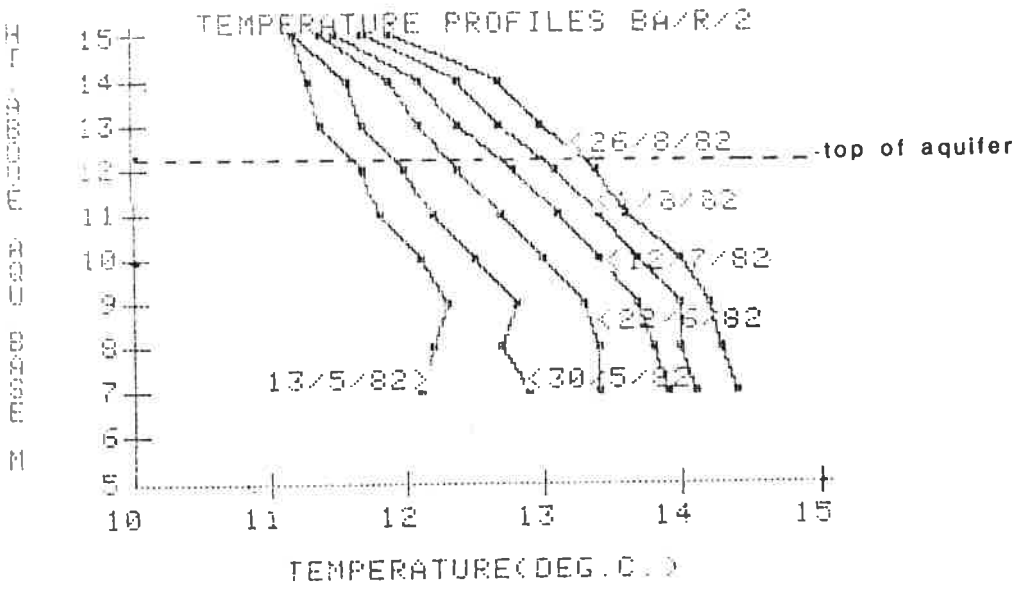

FIGURE 16. Temperature profiles in BA/R/2 (13 m from injection bore) during storage phase.

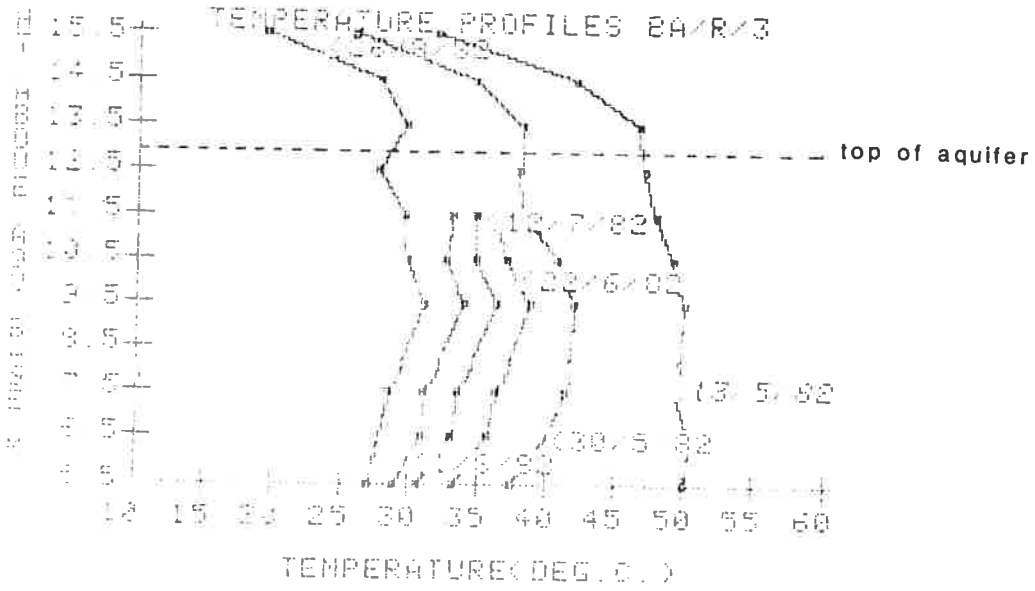

FIGURE 17. Temperature profiles in BA/R/3 (5 m from injection bore) during storage phase.

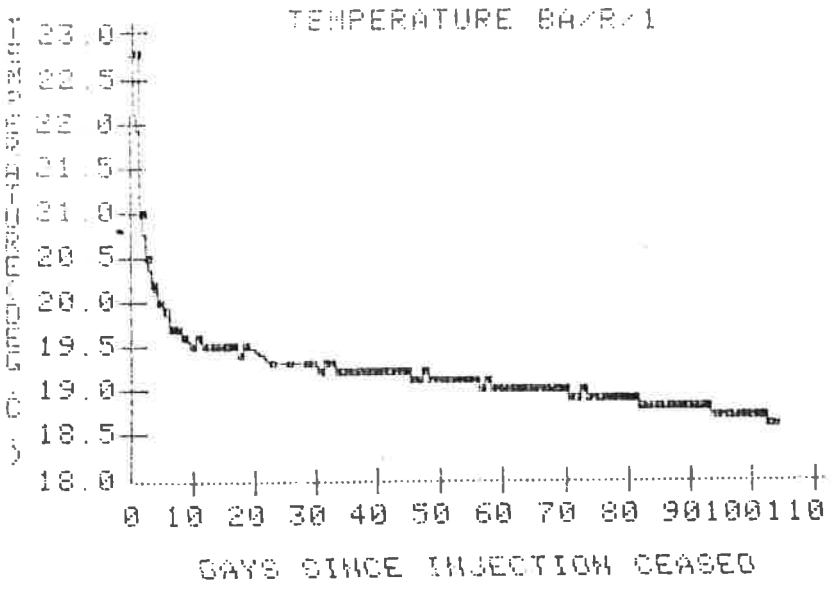

FIGURE 18. Temperature as a function of time in BA/R/1 (10 m from injection bore.) during storage phase.

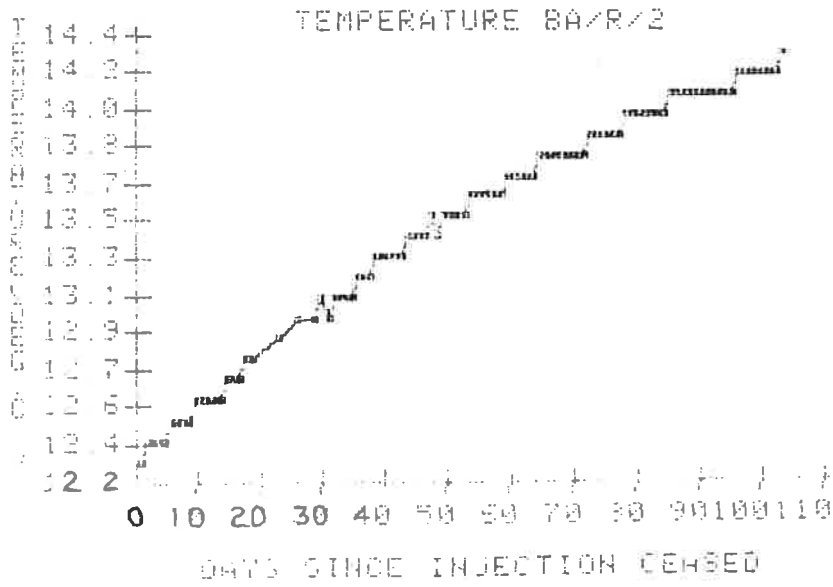

FIGURE 19. Temperature as a function of time in BA/R/2 (13 m from injection bore) during storage phase.

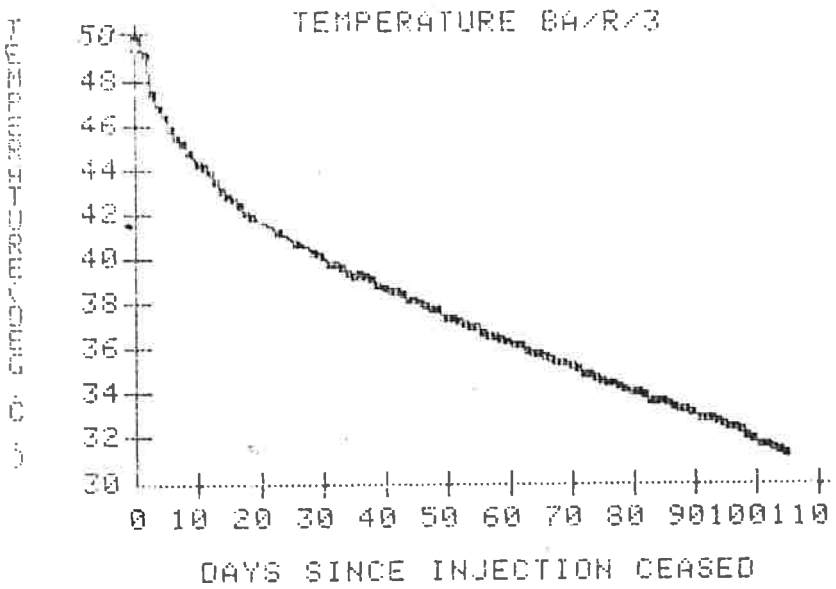

FIGURE 20. Temperature as a function of time in BA/R/3 (5 m from injection bore) during storage phase.

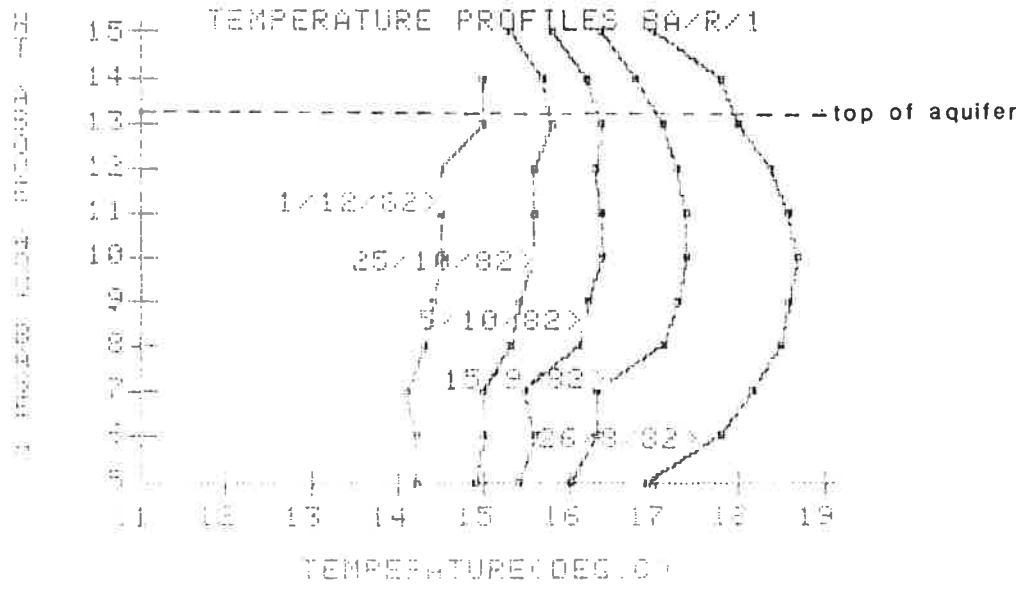

FIGURE 21. Temperature profiles in BA/R/1 (10 m from injection bore) during abstraction phase.

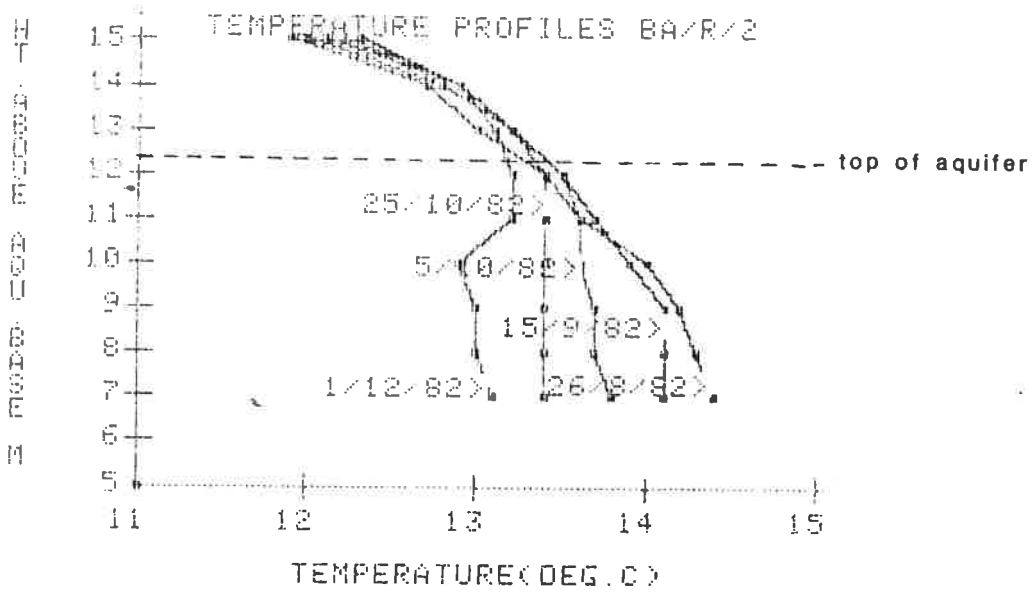

FIGURE 22. Temperature profiles in BA/R/2 (13 m from injection bore) during abstraction phase.

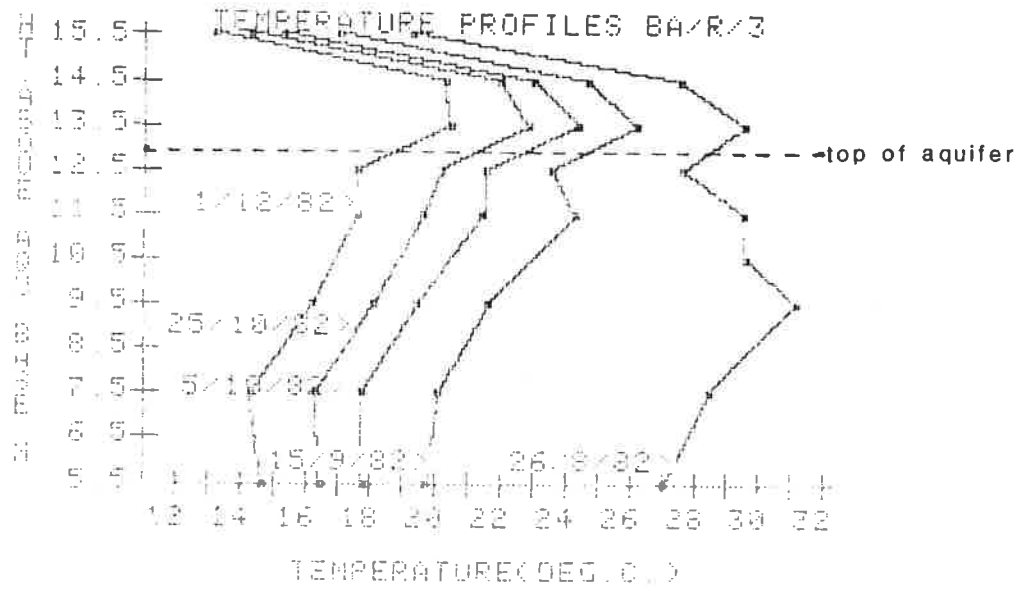

FIGURE 23. Temperature profiles in BA/R/3 (5 m from injection bore) during abstraction phase.

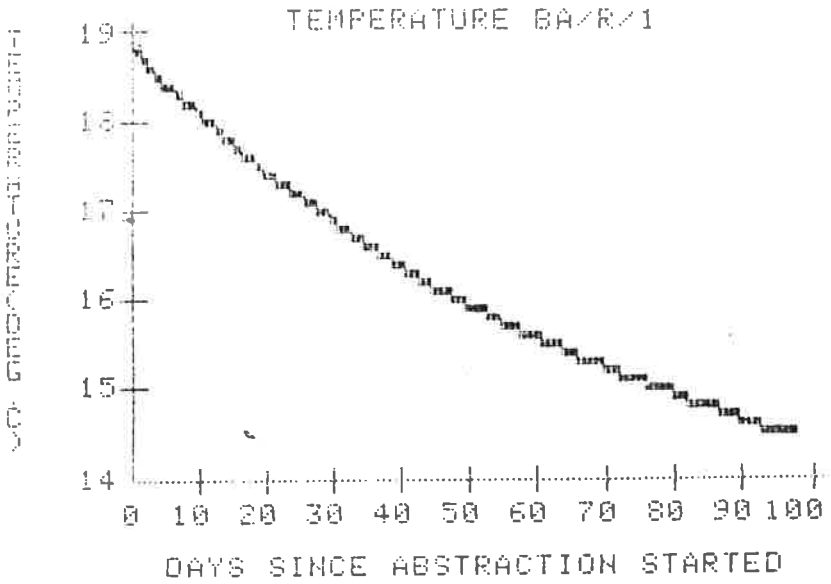

FIGURE24. Temperature as a function of time in BA/R/1 (10 m from injection bore) during abstraction phase.

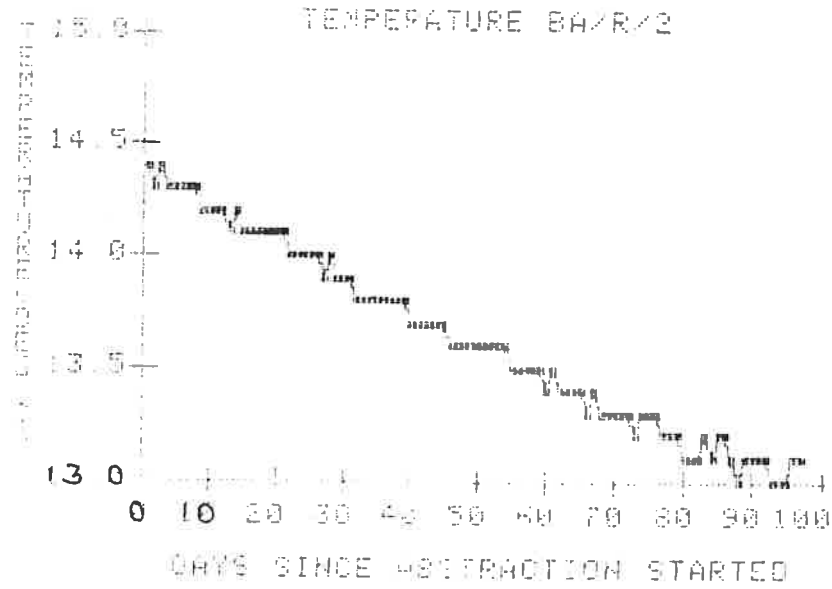

FIGURE 25. Temperature as a function of time in BA/R/2 (13 m from injection bore) during abstraction phase.

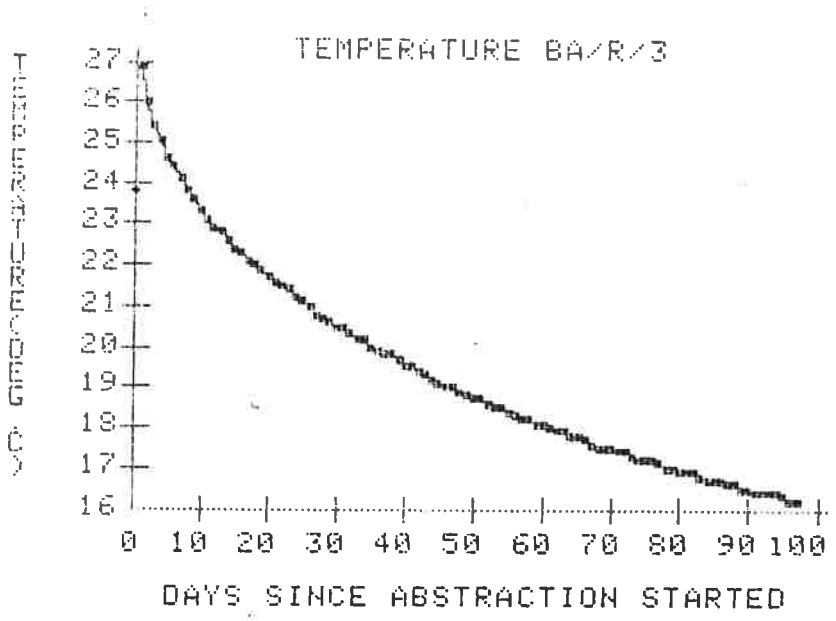

FIGURE 26. Temperature as a function of time in BA/R/3 (5 m from injection bore) during abstraction phase.

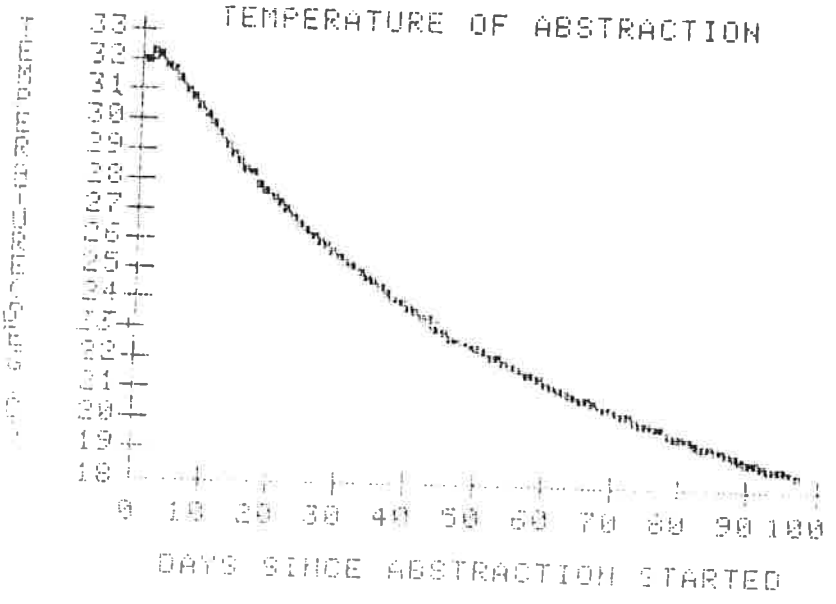

FIGURE 27. Temperature of abstracted water at well head as a function of time.

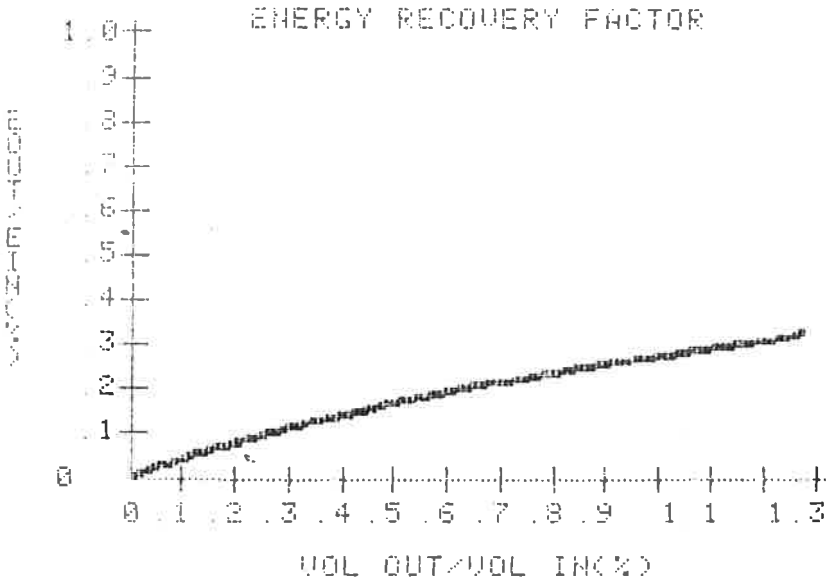

FIGURE 28. Energy recovered as a function of the proportion of the volume of injected water recovered.

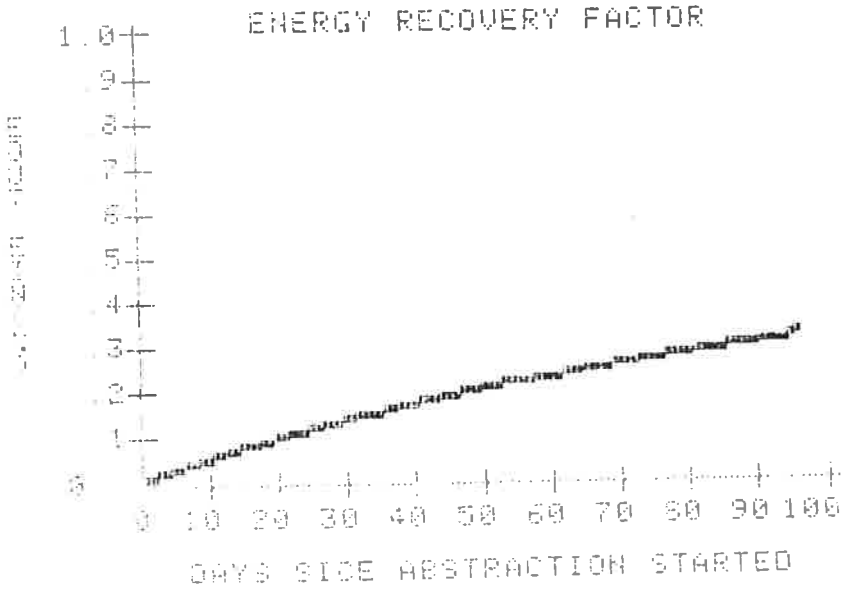

FIGURE 29. Energy recovered as a function of time.

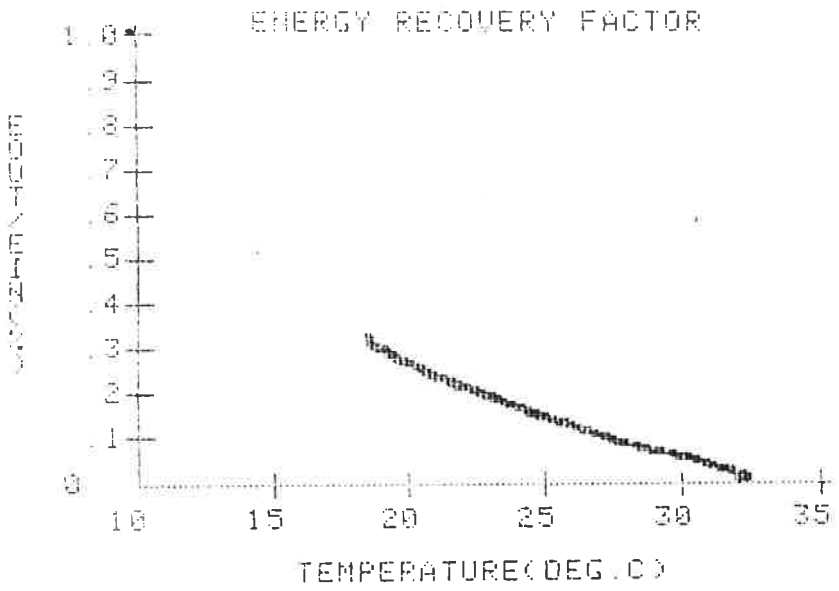

FIGURE 30. Energy recovered as a function of well-head temperature.

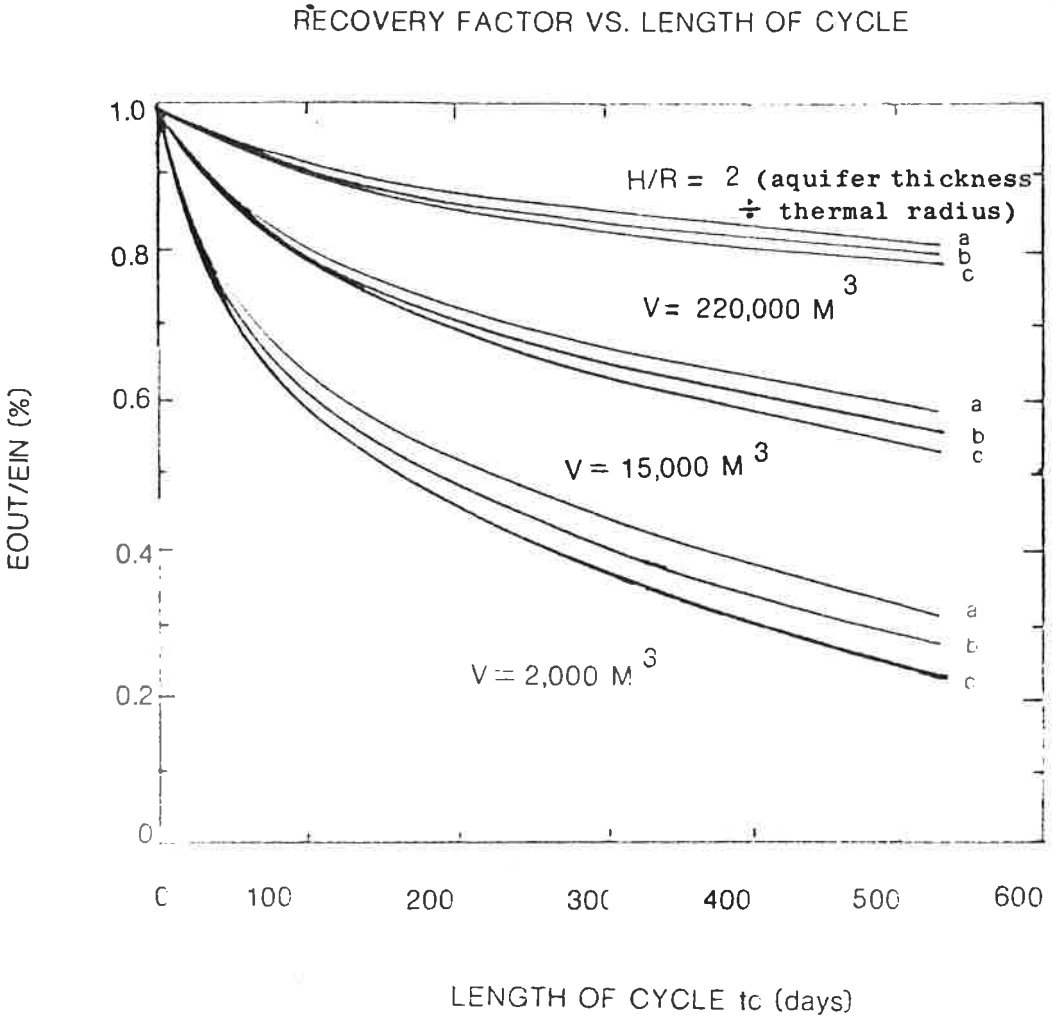

FIGURE 31. First cycle recovery factor versus cycle length for several injection-storage-production-rest schedules for three thermal volumes (after Doughty et al. 1982)

For a ti = tp = tc/2

For b ti = ts = tp = tr = tc/4

For c ts = tr = tc/2 ti = tp = 0

where ti = length of injection
ts = length of storage
tp = length of production
tr = length of rest
tc = length of whole cycle

APPENDIX A

The rise in temperature in the Chalk observation well due to horizontal conduction of heat through the saturated Chalk aquifer

The observed rise in temperature within the Chalk observation borehole during the injection phase could either be due to leakage of injection water into the Chalk aquifer or horizontal conduction of heat from the column of water above the packer in the injection borehole through the saturated Chalk or a combination of both. The 30 m thickness of Gault Clay with its poor thermal characteristics precludes conduction of heat vertically from the Lower Greensand. The purpose of this note is to determine the maximum possible temperature rise in the Chalk observation borehole due to horizontal conduction of heat from the column of water in BA/R/4 alone.

Using a function defined by Jaeger (1956) and reported by Hantush (1964) the temperature rise within the Chalk observation well due to conduction can be calculated.

The equation used is:

$$\frac{\theta\,(r,t) - \theta_o}{\theta_w - \theta_o} = A\left(\frac{t\,K}{r_w^2}\,,\ \frac{r}{r_w}\right)$$

where $\theta\,(r,t)$ is the temperature in the observation borehole at distance r from the injection borehole after time t.

θ_o is the initial groundwater temperature at time t_o

θ_w is the temperature of the column of water above the packer in the injection borehole at $t > t_o$

A is the function tabulated by Hantush (op. cit.)

r_w is the radius of the injection well

K is the diffusivity of the Chalk aquifer.

Fig. A1 shows the temperature recorded by the thermistor in the injection borehole above the packer, as a function of time. As an approximation the temperature of the column of water above the packer after the onset of injection is taken as a constant 42°C. Initial groundwater temperature is taken at 10°C. The radius of the injection borehole is 7.6 cm and the observation borehole is 105 cm from the injection borehole. For t = 79 days the value of function A is given as 0.28. Thus $\theta\,(r,t)$ for t = 79 days = 19.24°C which is a good approximation to the temperature within the Chalk observation borehole at the end of the injection period.

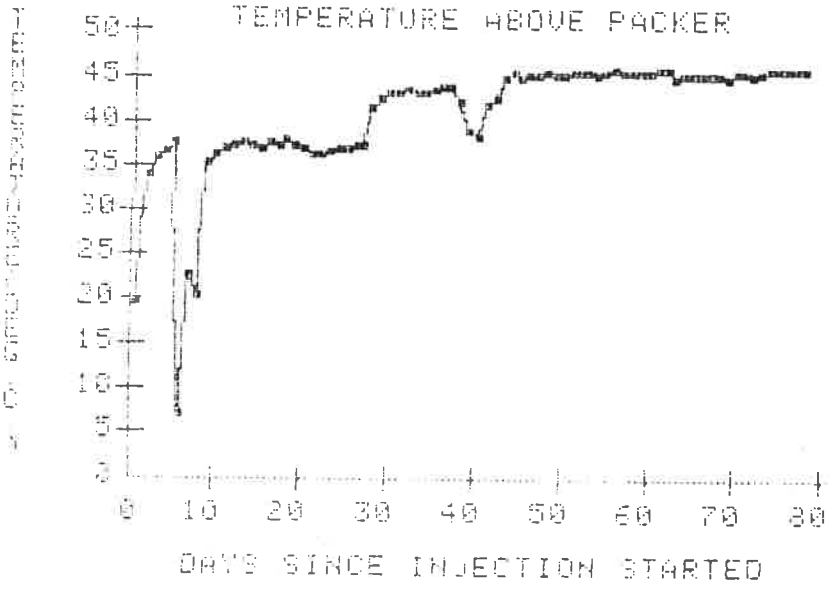

FIGURE A1. Temperature of water in the injection borehole above the packer.

APPENDIX B

Table of channels used on Kratos "Link On" units

KRATOS/APPLE CHANNEL REFERENCE NUMBERS

KRATOS NO.	10		11		12		13	
CHANNEL No ON LINKON	DA	DEVICE	DA	DEVICE	DA	DEVICE	DA	DEVICE
0	0	INTERFACE VOLTAGE	16	INTERFACE VOLTAGE	32		40	INTERFACE VOLTAGE
1	1	FLOWRATE UNISELECTOR	17	THERMISTOR BA/R/3 6	33		41	THERMISTOR BA/R/1 9
2	2	THERMISTOR ABOVE PACKER	18	" " 7	34		42	" " 10
3	3	THERMISTOR BA/R/4 1	19	" " 8	35	PRESS TRANS BA/R/4	43	" " 11
4	4	" " 2	20		36	" " BA/R/2	44	" " 12
5	5	" " 3	21	" " 10	37	ATMOSPHERIC PRESS.	45	THERMISTOR WELL HEAD
6	6	" " 4	22	" " 11	38	PRESS. TRANS BA/R/3	46	MID CHALK O.W. THERM.
7	7	" " 5	23	" " 12	39	PRESS. TRANS BA/R/1	47	THERMISTOR BA/R/2 4
8	8	" " 6	24	THERMISTOR BOT. CHALK O.W			48	" " 5
9	9	" " 7	25	THERMISTOR BA/R/1 2			49	" " 6
10	10	" " 8	26	" " 3			50	" " 7
11	11	THERMISTOR TOP CHALK O.W	27	" " 4			51	" " 8
12	12	THERMISTOR BA/R/3 2	28	" " 5			52	" " 9
13	13	" " 3	29	" " 6			53	" " 10
14	14	" " 4	30	" " 7			54	" " 11
15	15	" " 5	31	" " 8			55	" " 12

Note: (a) Each Kratos unit has 16 channels (0-15) except 12 which has 8 (0-7). In HEATSTORE nn the information from all Kratos Units on any one log is held in array DA(56) - the array elements being allocated as shown above.

(b) All thermistors in BA/R/4 had failed by the start of the abstraction phase. During the abstraction phase DA(3) and DA(4) were used for additional well head thermistors in the rising main.